Vol. 22: 95–110, 2014
doi: 10.3354/ab00586

AQUATIC BIOLOGY
Aquat Biol

Published November 20

Contribution to the Theme Section 'Environmental forcing of aquatic primary productivity'

Light acclimation and pH perturbations affect photosynthetic performance in *Chlorella* mass culture

Sven Ihnken[1,*], John Beardall[2], Jacco C. Kromkamp[1], Cintia Gómez Serrano[3], Moacir A. Torres[4], Jiří Masojídek[5], Irene Malpartida[3], Robert Abdala[3], Celia Gil Jerez[3], Jose R. Malapascua[5], Enrique Navarro[6], Rosa M. Rico[3], Eduardo Peralta[3], João P. Ferreira Ezequil[6,7], Félix Lopez Figueroa[3]

[1]Royal Netherlands Institute for Sea Research (NIOZ), PO Box 140, 4400 AC Yerseke, The Netherlands
[2]School of Biological Sciences, Monash University, Clayton, Victoria 3800, Australia
[3]Departamento de Ecología, Facultad de Ciencias, Universidad de Málaga, Campus Universitario de Teatinos s/n, 29071 Málaga, Spain
[4]Departamento de Bioquímica, Institute de Química, Unversidade de São Paulo, SP, Brazil
[5]Institute of Microbiology, Academy of Sciences, 37981 Trebon, Czech Republic
[6]Pyrenean Institute of Ecology (CSIC), Av. Montañana 1005, Zaragoza 50059, Spainl
[7]Departamento de Biologia, Universidade de Aveiro, Aveiro 3810-193, Portugal

ABSTRACT: *Chlorella* spp. are robust chlorophyte microalgal species frequently used in mass culture. The pH optimum for growth is close to neutrality; at this pH, theoretically little energy is required to maintain homeostasis. In the present study, we grew *Chlorella fusca* cells in an open, outdoor, thin-layer cascade photobioreactor (TLC), under ambient photon flux at the theoretically preferred pH (7.2), and let the culture pass the exponential growth phase. Using pH drift experiments, we show that an alkalization to pH 9 supported photosynthesis in the TLC. The increased photosynthetic activity under alkaline conditions was a pH-dependent effect, and not a dissolved inorganic carbon (DIC) concentration- or light intensity-dependent effect. Re-acidification (in one step or in increments) lowered gross oxygen production and increased non-photochemical quenching in short-term experiments. Gross oxygen production and electron transport rates in PSII were uncoupled during the pH perturbation experiments. Electron transport rates were only marginally affected by pH, whereas oxygen production rates decreased with acidification. Alternative electron pathways, electron donation at the plastid terminal oxidase and state-transitions are discussed as a potential explanation. Because cell material from the TLC was not operating at maximal capacity, we propose that alkalization can support photosynthesis in challenged TLC systems.

KEY WORDS: *Chlorella* · Mass culture · pH perturbance · Chlorophyll fluorescence · Oxygen production · pH drift · Photosynthesis · Photoprotection

INTRODUCTION

Scenescence and mass culture

Microalgae mass culture generally aims for high biomass yields, often associated with intended nutrient starvation to increase lipid contents (Jacobsen et al. 2010, Liu et al. 2013). Nitrogen starvation lowers protein contents, RuBisCO levels, and activates biochemical responses that lead to an elevation of lipid bodies by a process that is not entirely understood. Algae mass-culture conditions are frequently less controlled, the exponential growth phase might have passed during the time of cell harvest and cells have experienced senescence. Under these conditions cells can exhibit acclimation properties which are comparable to nutrient starvation conditions. Lower photosynthetic performance is one result of senes-

*Corresponding author: s.ihnken@gmail.com

Publisher: Inter-Research · www.int-res.com

cence (Humby et al. 2013). When cells enter the stationary growth phase, chloroplast structures become disorganized, LHCII, D1, PsaA, Cyt f, and RuBisCO levels decline, and photosynthesis is down-regulated while non-photochemical quenching (NPQ) remains stable compared to the exponential growth phase (Humby et al. 2013). These substantial changes within the chloroplast might affect the cell's response to external factors such as pH and light intensity. Gardner et al. (2011) showed that a *Chlorella* strain demonstrated elevated lipid contents and displayed morphological changes at high pH, which indicates that the elevated pH induced stress to the cell.

Homeostasis: effect of external pH manipulation

The external pH under which the cell is capable of operating at maximal capacity is species-specific but usually range between pH 6 and 8.5 (Taraldsvik & Mykleastad 2000, Hinga 2002, Lundholm et al. 2004, Liu et al. 2007, Middelboe & Hansen 2007). Although *Chlorella* spp. prefer a pH between 6 and 6.5 (Myers 1953), *Chlorella vulgaris* can grow effectively at an alkaline pH of 10.5 (Goldman et al. 1982). *Chlorella saccharophila* grows optimally at pH 7.0 but can maintain homeostasis when external pH is as low as 5.0 (internal pH 7.3) (Gehl & Colman 1985). This strain can successfully grow at pH 2.5 (Beardall 1981), which shows its immense internal pH regulation capacity. Internal pH is generally maintained within narrow limits above ~pH 7 in *Chlorella* (Smith & Raven 1979, Beardall & Raven 1981, Sianoudis et al. 1987) and other taxa (Dixon et al. 1989, Kurkdjian & Guern 1989). Homeostasis is maintained by 2 main processes: proton binding and H^+ translocation between cell organelles and the external medium by active, energy-demanding, or passive ion exchange mechanisms (Smith & Raven 1979). The energy demand for active proton translocation is estimated to be 1 ATP per H^+ transported (Briskin & Hanson 1992). The abundance of H^+ ATPase complexes can be controlled by the cell via pH sensing (Weiss & Pick 1996). However, Nielsen et al. (2007) showed that light intensity (and hence energy supply) did not correlate with cell growth under extreme pH conditions, which indicates that elevated light input does not necessarily enhance the cell's capacity to regulate internal pH. In short-term pH manipulations, H^+ pumping is important (Bethmann & Schönknecht 2009); however, under longer-term (growth) conditions, anion exchange might be the predominant proton translocation process (Lew 2010). It is not clear how internal pH is regulated in cells that have passed their exponential growth phase.

Carbon acquisition and pH

Changes in the media's pH or supplementation of CO_2 affects the bicarbonate equilibrium. Introducing CO_2 into the medium lowers the pH and shifts the bicarbonate equilibrium towards higher concentrations of CO_2 and bicarbonate at the expense of carbonate. If the pH is increased at a constant pCO_2, the dissolved inorganic carbon (DIC) concentration increases, while the $CO_{2(aq)}$:HCO_3^- ratio decreases. The form of DIC is relevant for the cellular DIC acquisition system, while the concentration of DIC matters when substantial rates of photosynthesis must be sustained. Most aquatic primary producers possess means of elevating the CO_2 concentration at RuBisCO, which suppresses RuBisCO's oxygenase function and provides sufficient CO_2 even when high photon flux (PF) allows high CO_2 fixation rates in the Calvin-Benson-Bassham-cycle. Most algae can regulate these CO_2-concentrating mechanisms (CCMs) effectively (Giordano et al. 2005). *Chlorella* spp. possess effective CCMs and acquire both CO_2 and/or HCO_3^- actively (Shelp & Canvin 1980, Beardall 1981, Beardall & Raven 1981), and are able to raise the pH in a closed vessel to pH 11 (Myers 1953), which shows that cells are capable of carrying out effective photosynthesis. The interlinked pH and CO_2 concentration behavior makes it difficult to separate both effects.

In the present study, we tested *Chlorella fusca* cells grown in an open, outdoor, thin-layer cascade photobioreactor (TLC) under post-exponential growth phase conditions. We investigated if cells are susceptible to high PF, are limited by external DIC concentrations or affected by changes in the medium pH. We perturbed pH in short-term (i.e. minutes) and long-term (i.e. hours: pH drift) experiments to test the cells' capacity to regulate pH-related photosynthesis. The results show that cells performed better in alkaline conditions and were stressed by acidification of the media.

MATERIALS AND METHODS

Organism, growth conditions and growth history

The chlorophyte microalga *Chlorella fusca* (Culture Collection of Marine Microalgae, ICMAN-CSIC, Cádiz, Spain) was grown in an outdoor thin-layer

cascade photobioreactor (TLC3; TLC number is given to enable comparison with to other studies using the same experimental setup) in September 2012 in southern Spain (Málaga), using Bold's Basal Medium modified with 3-fold nitrate content plus the addition of vitamins (3N-BBM-V) (Andersen et al. 2005). The cell suspension was held in an open tank (~120 l), pumped to the top of a flat panel slide (4 m^2, 2% inclination), and allowed to flow back to the tank by gravity (surface to volume ratio 27 m^{-3}, 145 l working volume). The cells received full sunlight on the cascade (for a duration of ~11 s) and were exposed to low light conditions in the tank. Completion of a single cycle took approximately 70 s. Macronutrients ($NaNO_3$, $MgSO_4$ and KH_2PO_4) were added once a day using common farming fertilisers (Welgro Hydroponic, Comercial Química Massó); nutrient concentrations were ≥540 mg l^{-1} (PO_4^- and SO_4), and ≥650 mg l^{-1} (NO_3^-; R. Abdala pers. obs.). The TLC was aerated; pure CO_2 gas was injected into the air stream (final 1%) and the pH was maintained at between 7.2 and 7.6. pH drift experiments showed very limited capacity of the cells to increase the pH by means of photosynthesis (see Fig. 1A), even when DIC was added in form of $NaHCO_3$ (see Fig. A1A in the Appendix), or when diluted with fresh medium (Fig. A1C). We therefore tested the photophysiological fitness in a light acclimation experiment (see Figs. 2 & 3), which showed that photosynthetic capacity was not severely impaired. However, increasing the pH by substantial addition of $NaHCO_3$ (20 mM) in the TLC increased pH drift (see Fig. 1). pH perturbance experiments were carried out after pH adjustments had been performed in the TLC. Cell numbers decreased for 2 d prior to the experiments (see Figs. 4–7) (from ~1 × 10^6 to ~4 × 10^5 cells ml^{-1}), but remained stable thereafter (counted using a Neubauer chamber; R. Abdala pers. obs.). At that point, the TLC had been maintained for 12 d, at a temperature of ~25°C. The TLC used in the present study was part of a nutrient-concentration effect study. A TLC with replete nutrients concentrations (TLC presented in the present study), was maintained parallel to a TLC with low nitrogen (TLC–N) and another TLC with lowered sulphate concentrations (TLC–S). We expected the TLC with replete nutrients to show highest cell numbers. However, maximal cell concentrations were lower than expected (TLC of the present study, i.e. replete nutrients = 2 × 10^7 cells ml^{-1}, TLC–S = 2.3 × 10^7 cells ml^{-1}, and TLC–N = 1 × 10^6 cells $m^{-1}l$; R. Abdala pers. comm.). The experiments in the present study were carried out after the maximal TLC capacity had passed, and cell suspensions experienced grazing, grazer treatment and were contaminated with *Nannochloris* sp. and *Chlamydomonas* sp. cells in variable concentrations.

More information about the hydrodynamics of the TLC used and light exposure effects in the TLC on photosynthetic performance is given in Jerez (2014, this Theme Section). Further information on photoacclimation in the TLC will be published elsewhere (J. C. Kromkamp et al. unpubl.).

pH drift experiments

Samples were withdrawn from the TLC in the morning, transferred to 20 ml glass scintillation vials, and either continuously exposed to ambient sunlight or shaded by neutral density filters. pH was measured several times a day (Basic 20, Crison Instruments), calibrated with standard laboratory solutions. Measurement duration was standardized to 1 min $vial^{-1}$ to avoid erratic gas exchange amongst replications. Temperatures were in the range of 25 to 28°C and maintained by placing vials in a non-controlled tub water bath and regularly exchanging the cooling fluid.

Light acclimation experiment

Cell suspensions for continuous light exposure experiments were withdrawn from the TLC in the evening. 250 ml were filled into 500 ml conical glass flasks, which were kept in the dark overnight and then exposed to ambient light conditions (HL, high light) the following day while aerated with ambient air (~1 l min^{-1}). Shading was achieved by neutral density filters to 70% (ML, medium light) or 30% (LL, low light) of the ambient PF. Temperature conditions were maintained at approximately 25 ± 3°C by placing flasks in a styrofoam tub filled to one-third with water (which was replaced when needed). At given times, 2 ml samples were withdrawn, immediately placed in an AquaPen fluorometer (AquaPen, P.S.I.) and fast fluorescence induction curves measured. Maximum and effective quantum yield of PSII (F_v/F_m and F_v'/F_m') and Vj (accumulation of the 'primary' acceptor of PSII, Q_A^-) were computed by the software provided by the instrument. Initial samples were dark-incubated overnight. Other samples were measured in the absence of actinic light, which allows Q_A^- to oxidize. However, because samples were not dark-acclimated prior to measurements, nor exposed to ambient actinic light, residual NPQ can lower the fluorescence signal and decrease variable fluorescence. This results in F_0' dur-

ing the O phase of the fast fluorescence induction curve, rather than F' or F_0 (i.e. quantum yields are F_v'/F_m' rather than $\Delta F/F_m'$) (van Kooten & Snel 1990, Kromkamp & Forster 2003).

Fast fluorescence induction curves

Fast fluorescence induction curves represent the consecutive reduction of electron carriers in PSII and the plastoquinone (PQ) pool within about 1 s of illumination with saturating light. After the O phase (first data point at $t = 50$ µs), Q_A gets reduced until the J phase is reached (100% Q_A^-, 0% Q_A, 2 ms), while the consecutive reduction of Q_B and formation of plastoquinol (PQ pool reduction) is associated with the inflection (I phase) and the maximal fluorescence signal (P phase at $t = 1$ s) by a fully reduced electron transport chain from the PSII reaction centre to the PQ pool (Tomek et al. 2001, Zhu et al. 2005). This concept is commonly accepted, however, alternative interpretation of fast fluorescence induction curves have been frequently presented due to the high number of fluorescence quenchers in PSII and the photosynthetic unit (Strasser et al. 1995, Bukhov et al. 2004, Stirbet & Govindjee 2012). The reduction state of the PQ pool, for instance, was not a determinant factor for maximal fluorescence signals during P, but the reduced PQ pool has been shown to affect the J phase (Tóth et al. 2005, 2007). Nevertheless, we will interpret data of this study following Zhu et al. (2005), where signals show the accumulation of the following electron carrier: J phase = Q_A^-, P phase = Q_A^- Q_B^{2-}, PQ is fully reduced. Vj was calculated as (J − O) / (P − O), with J phase = F_{2ms} (where F = fluorescence), O = $F_{50\mu s}$, P = F_{1s}. 1 − Vj is indicative for the electron transport capacity past Q_A. Low values represent a lower probability that electrons are efficiently transported. Note that P = F_m (or F_m') in multiple-turnover saturation pulse fluorometers (e.g. pulse-amplitude modulation, PAM), while J is equivalent to maximal fluorescence in a single-turnover fluorometer (e.g. fast repetition rate fluorometer, FRRf).

pH perturbations: simultaneous PAM, O_2 and pH measurements

Cell suspensions were withdrawn from the TLC and placed in a 20 ml glass scintillation vial. The lid was modified to allow submersion of a standard pH electrode (Basic 20, Crison Instruments), and an oxygen optode (Microx TX3 PreSens) into the cell suspension, while minimizing the contact surface of the cell suspension with ambient air. The optical fibre of a Mini-PAM (Walz) was placed against the top one-third of the vial and orientated perpendicular to the actinic (white LED) light source, which provided a constant PF of 140 µmol photons m^{-2} s^{-1}. Higher actinic PF was achieved by usage of the internal light source of the fluorometer and exposed cells to 400 µmol photons m^{-2} s^{-1} when switched on. However, cells moved into and out of the additional light field since only a part of the scintillation vial was exposed to the additional PF. This can limit comparison with the FRRf experiment, where the entire volume of the cell suspension was exposed to PF conditions. Cell suspensions were stirred continuously. After a ~4 min acclimation phase, additions of known amounts of HCl perturbed the pH, which was recorded manually every 30 s. To test for DIC limitation, 300 µl of $NaHCO_3$ (1 mM final concentration) were injected at the times indicated. Experiments were conducted from morning until noon, before high ambient light could cause inhibition.

pH perturbations: fast repetition rate fluorescence measurements

FRRf fluorometers use a different excitation and measurement protocol compared to PAM instruments. While PAM measures F_m or F_m', during a multiple turnover (of PSII) saturation pulse (approx. 800 ms duration), FRRf uses a sequence of subsaturating flashlets to consecutively reduce PSII to a single turnover. The FRR fluorometer used (FastTracka Mark II, Chelsea Technology Group) was equipped with a bench-top illumination extension (FastAct, Chelsea Technology Group) and was set to apply a sequence of 100 flashlets, each 1 µs long and spaced 50 µs apart. Data from 12 such sequences were averaged by the standard FRRf software (FastPro) and produced quantum yields (F_v/F_m, $\Delta F/F_m'$) of a single turnover in PSII, i.e. all Q_A reduced, PQ-pool not affected. An iterative curve fit of a single excitation flashlet sequence provides measurements of the functional absorption cross-section of PSII (in nm^2). A sequence of single measuring flashlets after the single turnover excitation protocol shows Q_A^- re-oxidation kinetics (τ_{PSII}), i.e. the electron transport capacity from a fully reduced Q_A. Further information about FRRf fluorometry can be found in Kolber & Falkowski (1992, 1993) and Kolber et al. (1998).

A total of 3 ml of microalgae culture was withdrawn from the TLC on the same day as PAM pH

perturbation experiments were carried out, and immediately placed in the FRR fluorometer. An internal LED provided actinic PF of 3, 140, 400, 140 and 0 µmol photons m^{-2} s^{-1} in this sequence for the times indicated. Acidification 5 min after the start of the protocol was achieved by addition of 8.6 µl of 0.5 M HCl. After 7 min, the pH was brought back up by injection of 51 µl 0.1 M NaOH. Samples were homogenized by aeration between each saturation flashlet application, which enables gas exchange between the cell suspension and air, and complicates data interpretation regarding the bicarbonate system and pH.

RESULTS

pH drift experiments

pH drift was monitored daily. Until the pH was increased in the TLC, incubations could elevate the pH by a maximum of 0.5 pH units (examples are given in Fig. A1 in the Appendix). To test if cells were DIC limited, we added small amounts of DIC (400 and 800 mM), which increased the initial value (pH 7.11) marginally (pH 0.06 and 0.23 units respectively). Incubations with increased DIC concentrations showed similar pH rise kinetics compared to the control (Fig. A1A,B). pH drift experiments where fresh media was added to cell suspensions from the TLC (1:1 by volume) did not stimulate pH drift compared to the control, neither did CO_2 bubbling performed before the experiment (Fig. A1C). This indicates that cells were not nutrient starved or depleted. When the pH in the TLC was adjusted (from pH 7 to 9), pH drift increased (initial pH 8.47, final pH 9.57; Fig. 1). No pH increase was recorded in suspensions collected before the DIC addition. A stronger pH drift was observed on the following day (initial pH 8.65, final pH 11.5 ± 0.06; Fig. 1B). A similar effect was previously observed in another TLC (TLC2) (S. Ihnken pers.obs., J. C. Kromkamp et al. unpubl.), where the pH was increased from pH 7 to 8.5 and drift experiments showed increased pH rise (initial pH 8.5, final pH 10.5).

Fig. 1B shows that shielding the vials at 70% of ambient PF (i.e. ML) resulted in the highest final pH. Higher and lower PF levels showed a similar pH drift capacity, with some variation due to photoinhibition (HL), or light limitation (LL). Control flasks, which experienced the same treatment but remained closed for the entire period, showed similar final pH values compared to vials that were used for pH measurements, indicating that the measurements and the accompanying brief exposure to air did not influence the results. In samples which experienced full ambient PF (HL), however, a lower final pH was found in the control vials (pH 11.09 ± 0.25 and pH 10.02 ± 0.18 for opened and continuously closed vials respectively).

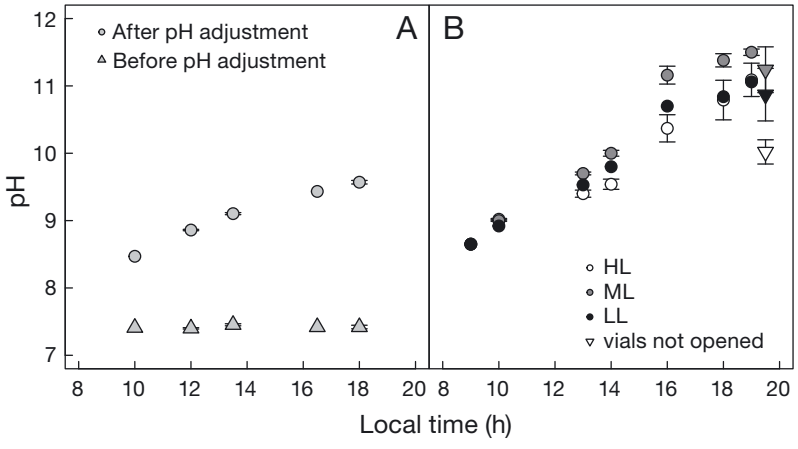

Fig. 1. pH drift experiments with *Chlorella fusca* cells collected (A) before and after the pH was increased by addition of $NaHCO_3^-$ in the thin-layer cascade photobioreactor (TLC) (refer to 'Results' section for DIC-effects versus pH-effects). (B) Light intensity effect on pH-adjusted suspensions to full-strength ambient photon flux (HL), medium light (ML: 70% of ambient photon flux), and low light (LL: 30%). Cells were collected from the TLC in the morning, and exposed to natural sunlight throughout the day. Glass scintillation vials shielded cells from a high fraction of UV light. Vials in (A) were shaded to ML levels. Temperature was kept below 28°C. Data show means ± SD when plot symbol is extended (n = 3). Times are given in 24 h format

Light acclimation status

Fig. 2 shows the light acclimation capacities in a separate experiment where cells were withdrawn from the TLC and continuously exposed to ambient PF. F_v'/F_m' decreased with increasing ambient PF in all treatments. The lowest quantum yields were found in full light exposed samples after the highest ambient PF, while ML cells had already started to recover at this point (t = 15:00 h). HL cells recovered from low midday yields in the evening. LL cells lowered values only marginally around noon. F_v'/F_m' depressions in HL and ML samples were partly caused by impairment of electron transport capacities past Q_A. 1 – Vj decreased by 1 unit at the highest PF, but recovered later during the day (Fig. 2B). Low re-oxidation turnover

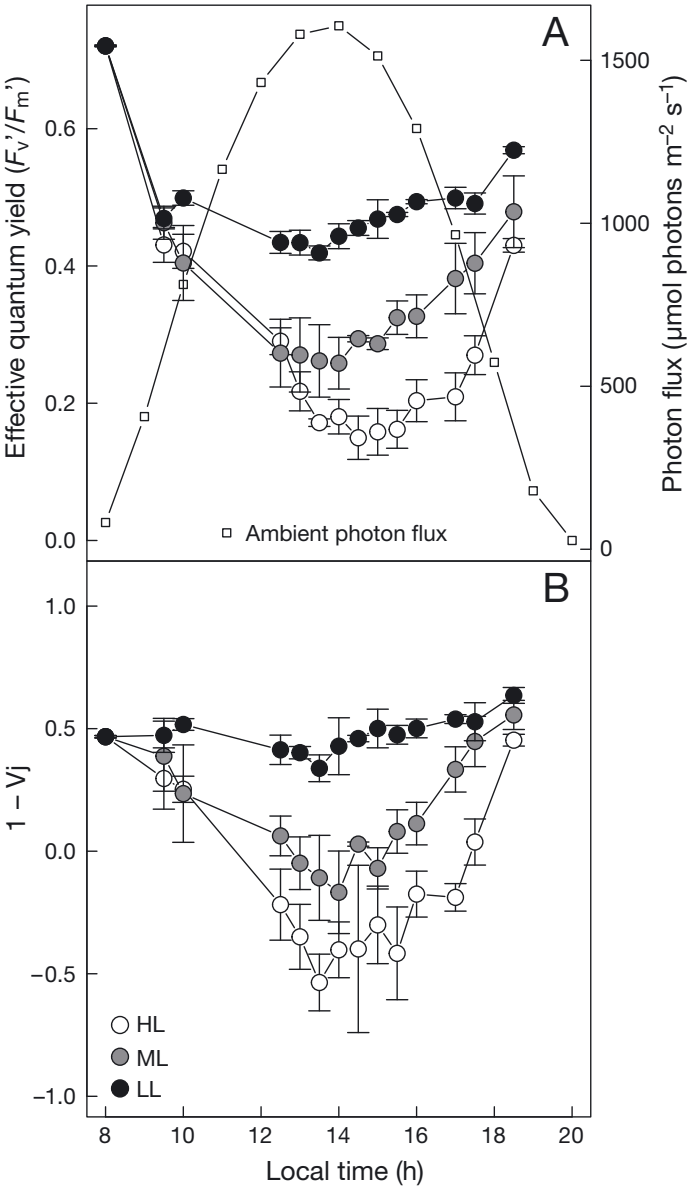

Fig. 2. *Chlorella fusca*. Photosynthetic parameters calculated from fast fluorescence induction curves shown in Fig. 3. Samples were withdrawn from the TLC and continuously exposed to HL, ML or LL (see Fig. 1). Data show (A) effective quantum yields and hourly averaged photon flux and (B) Q_B redox parameter 1 – Vj. Samples were dark-acclimated for ≤2 s before measurements were performed. Effective quantum yields are therefore denoted as F_v'/F_m' ($[F_m' - F_o'] / F_m'$ and not $\Delta F/F_m'$, which requires application of a saturation pulse under actinic irradiance). Efficient quantum yields are indicative of the efficiency of photon usage for photosynthetic electron transport. 1 – Vj represents the probability that an electron in Q_A^- moves further to electron carriers including the plastoquinone (PQ) pool. The higher the value (efficient F_v'/F_m', or 1 – Vj), the higher the photosynthetic competence of the sample. Data show mean ± SD (n = 3; n = 2 for fluorescence induction curves shown in HL for t > 15:00 h; where n = 2 due to failure of aeration in 1 replicate)

for electron carriers past Q_A, as shown by 1 – Vj, were also visible in low P phase values during the fast fluorescence induction in HL samples (Fig. 3). The lowest P phase values were found in the afternoon (15:00 h, HL), but samples recovered thereafter. J phase signals were only repressed in HL samples but remained low in the evening. In LL samples, the J phase was hardly affected; however, P phase values increased over the course of the day, with higher values in the evening than in the morning.

To test if cells suffered from DIC limitation, samples were withdrawn from the experiment (Fig. 3) at 3 times (morning, noon, afternoon), exposed to actinic PF of approximately 140 µmol photons m^{-2} s^{-1} for 2 min, spiked with DIC to a final concentration of 300 µM, and $\Delta F/F_m'$ followed for 4 min by a Mini-PAM. $\Delta F/F_m'$ was not enhanced by DIC additions (see Fig. A2 in the Appendix).

pH perturbation: decreasing pH

Perturbation experiments were carried out with subsamples of the TLC, 2 d after the pH was increased from ~7.2 to ~9. Acidification of the medium lowered the fluorescence signal rapidly (Fig. 4A). Both F' (i.e. steady-state fluorescence under actinic light conditions) and F_m' (maximal fluorescence measured during a saturation pulse by the fluorometer) decreased within approximately 1 s to a lower state when the pH was dropped. Continuously recorded fluorescence signals indicate a recovery from acidification, as can be seen by a slow increase in F' and F_m' until the pH was raised. The decrease in F_m' was caused by a rapid increase in NPQ. However, lower pH did not affect relative electron transport rates (rETR) effectively; values remained stable after HCl additions.

Acidification decreased gross oxygen evolution from 11.2 ± 1.74 to 3.7 ± 2.61 µM l^{-1} min^{-1} (data averaged from Figs. 4 & 5). This is surprising as fluorescence measurements suggest a steady continuation of rETR. Acidification therefore led to an uncoupling of oxygen and variable fluorescence based measurements of photosynthesis.

Supplementing suspensions with DIC (1 mM) did not increase rETR. Photosynthetic O_2 production, however, appeared to be stimulated in 1 sample when the DIC amendment was performed under acidic conditions, but not in another (Fig. 4B but not C). Cells of the different TLCs were tested regularly for DIC limitation where the photosynthetic performance remained unaffected by DIC additions at low or high growth pH (data not shown).

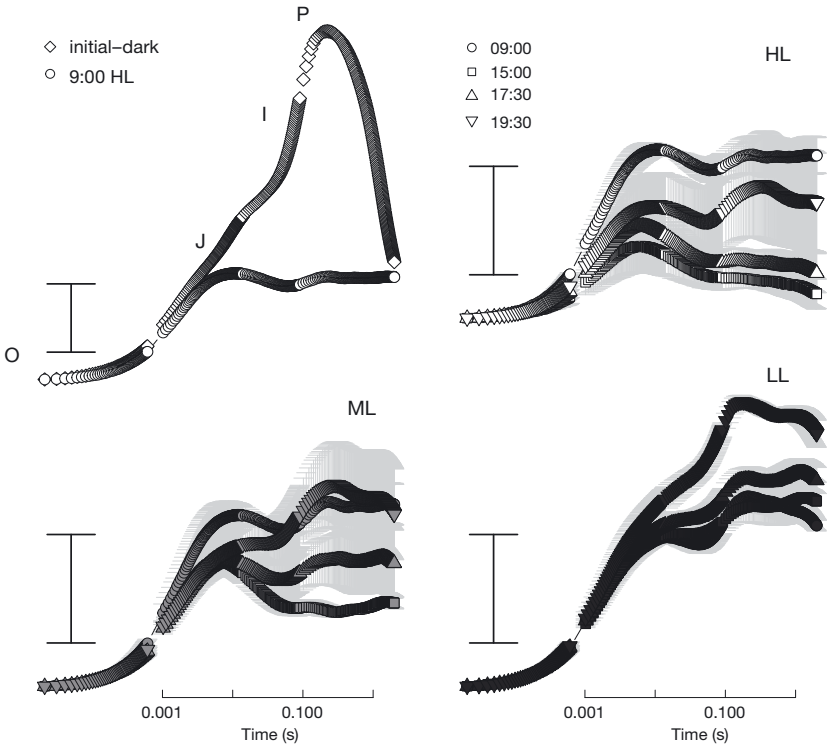

Fig. 3. Fast fluorescence induction curves of *Chlorella fusca* cell suspensions continuously exposed to HL, ML and LL (see Fig. 1) at different times of the day. A 250 ml cell suspension was withdrawn from the TLC, filled in 500 ml conical glass flasks, bubbled over night and exposed to measurement conditions on the following day. Samples were withdrawn from experimental conditions and dark-acclimated for ≤2 s before the measurement was performed. Data were normalized to O (initial fluorescence at t = 50 µs); vertical bars range over 0.5 units. Data show mean ± SD (n = 3; n = 2 for fluorescence induction curves shown in HL for t > 15:00 h where n = 2 due to failure of aeration in one replicate)

pH perturbation: increasing pH

Increasing the pH rapidly increased F' and F_m' to initial values or higher (Fig. 4). As a result, NPQ decreased to initial levels or lower. Negative NPQ values occurred when initial F_m' was lower than F_m' after the pH treatment. Because NPQ was calculated using the first F_m' value instead of F_m, negative NPQ values can occur, and indicate a lower NPQ state compared to values at the start of the experimental protocol. Photosynthesis measured by rETR was not affected by the single-step pH increase. Photosynthetic oxygen production, however, was stimulated by addition of NaOH. Initial values were not quite restored, which could have been be due to high oxygen concentrations in the vials at the end of the measurements due to a buildup of O_2 by photosynthesis.

Photon flux effect at low and high pH

When the actinic PF was increased 4-fold at low pH, rETR slowly increased during the entire period of elevated PF (Fig. 5). Decreasing F_m' values caused NPQ to increase until the pH was raised after 5 min. pH elevation caused a similar response under high PF conditions compared to low PF conditions (Fig. 4). PF elevation after cells were exposed to pH shifts did not induce a different response compared to PF elevation at low pH (Figs. 4 & 5). No pattern was found for oxygen production rates regarding PF.

Gradual pH amendments

When the pH was incrementally lowered, continuously recorded fluorescence and NPQ acclimation was visible (Fig. 6) in contrast to single-step pH perturbations, where very little acclimation was visible. Acclimation to pH increments was visible at pH >7.0, where alkalization increased the fluorescence signal, decreased NPQ and elevated oxygen production with highest values between pH 7 and 8. Gradual increase of pH mirrored responses to decreasing pH. Clearly, F' decreased with acidification, and increased with alkalization.

High time resolution measurements by FRRf

Fig. 7 shows variable fluorescence responses to pH perturbations in different PF levels. After a 3 min relaxation phase in very low light, the low actinic light (140 µmol photons m^{-2} s^{-1}) was switched on and led to a temporary increase in F' and F_m' followed by a drop and a quasi-steady state just before HCl was added (Fig. 7, dashed line), which decreased F' and F_m' further. NPQ was activated when the actinic light was switched on and reached maximum values briefly after acidification. rETR, however, was only marginally disturbed, which corroborates PAM measurements. The cells started to recover from acid addition within approximately 40 s, as shown by NPQ down-regulation. Increasing the actinic light

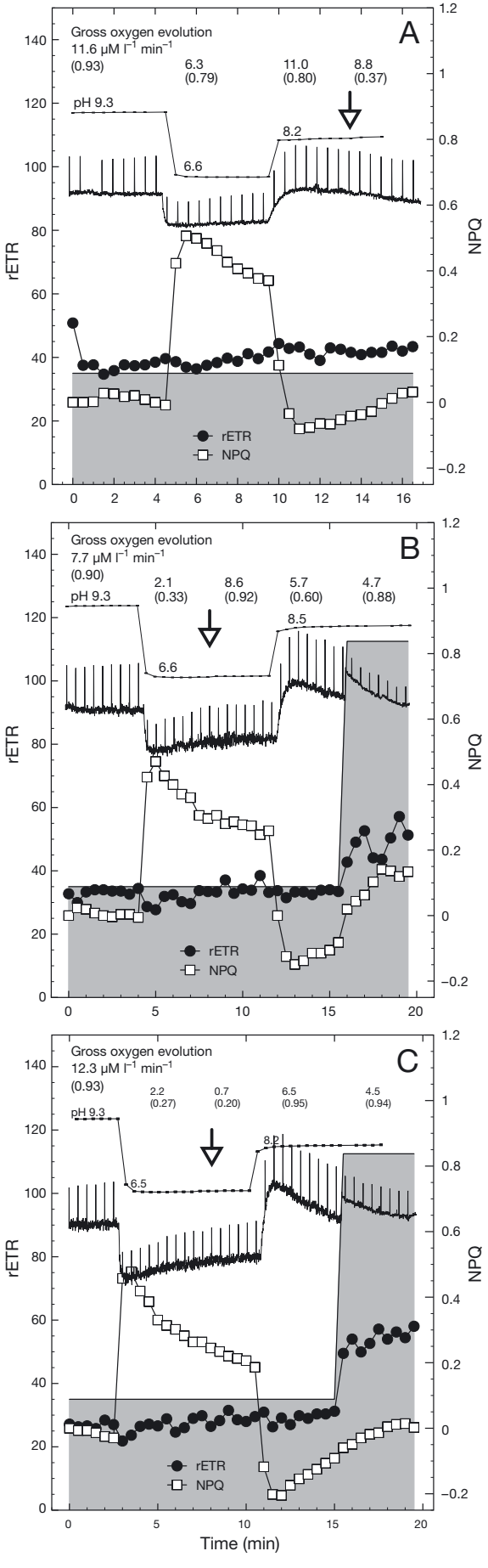

Fig. 4. *Chlorella fusca*. Photosynthesis and photoprotection in response to rapid pH perturbations. From to top to bottom in each panel, data show gross O_2 evolution and correlation coefficient (in brackets), pH, continuous fluorescence recording, non-photochemical quenching (NPQ), relative electron transport rates (rETR) and actinic photon flux (grey shaded area; 140 µmol photons m^{-2} s^{-1} in the low photon flux, LL, phase; 450 µmol photons m^{-2} s^{-1} in the high PF, HL, phase) measured simultaneously. rETR and photoprotection NPQ were determined using variable fluorescence with rETR = $\Delta F/F_m'$ × photon flux, and NPQ = ($F_m'^{\star}$ − F_m') / F_m', where $F_m'^{\star}$ = the first F_m' value of the experimental protocol. F_m was not measured as cells were not transferred to the dark prior to measurements. Data show responses to pH amendment at (A) constant photon flux, while in (B) and (C) the light intensity was increased at the end of the protocol. (C) shows a repeat measurement from (B) for error estimation purpose. pH perturbations were achieved by addition of small volumes (≤300 µl) of acid (HCl) or base (NaOH). DIC ($NaHCO_3^-$ solution) was added as indicated by arrows to yield final 1 mM. Note that continuous fluorescence lines, pH and oxygen concentrations do not read on any *y*-axis. pH was measured every 30 s

intensity to 400 µmol photons m^{-2} s^{-1} (Fig. 7, light grey bars) perturbed the NPQ down-regulation only briefly (~1 min). rETR clearly increased under additional light, but was down-regulated upon addition of NaOH and consequent rise of the pH. This is in contrast to PAM measurements, where rETR remained stable upon an alkalization at high PF (Fig. 5). Acidification and alkalization appears to induce 2 phases, one immediately after the pH adjustment for a duration of approximately 1 min. In the secondary phase, the parameters F', F_m' and NPQ developed in the opposite direction until the conditions were altered following the measurement protocol.

When cells were transferred to lower actinic PF, the effective quantum yields increased, mainly due to a relaxation of NPQ as F' increased only slightly. In a brief dark period, F' decreased to initial values and F_m' responded marginally, suggesting that photoprotective mechanisms were not active at the last light phase of the experimental protocol. Photoinhibition was absent, as shown by F_v/F_m values which were not repressed by the experimental treatment (0.37 ± 0.08 and 0.37 ± 0.07 for the first and last quantum yield respectively). While acidification lowered Q_A^- re-oxidation kinetics (τ_{PSII}) only slightly, addition of NaOH increased τ_{PSII} almost 2-fold (Fig. 7 C), which suggests a Q_A^- re-oxidation acceleration. The PSII functional cross section (σ_{PSII}) decreased when the actinic PF of 140 µmol photons m^{-2} s^{-1} was switched on due to a NPQ decrease. Acidification caused a slow rise in σ'_{PSII} until initial values were restored. The increase of the PF from 140 to 400 µmol photons

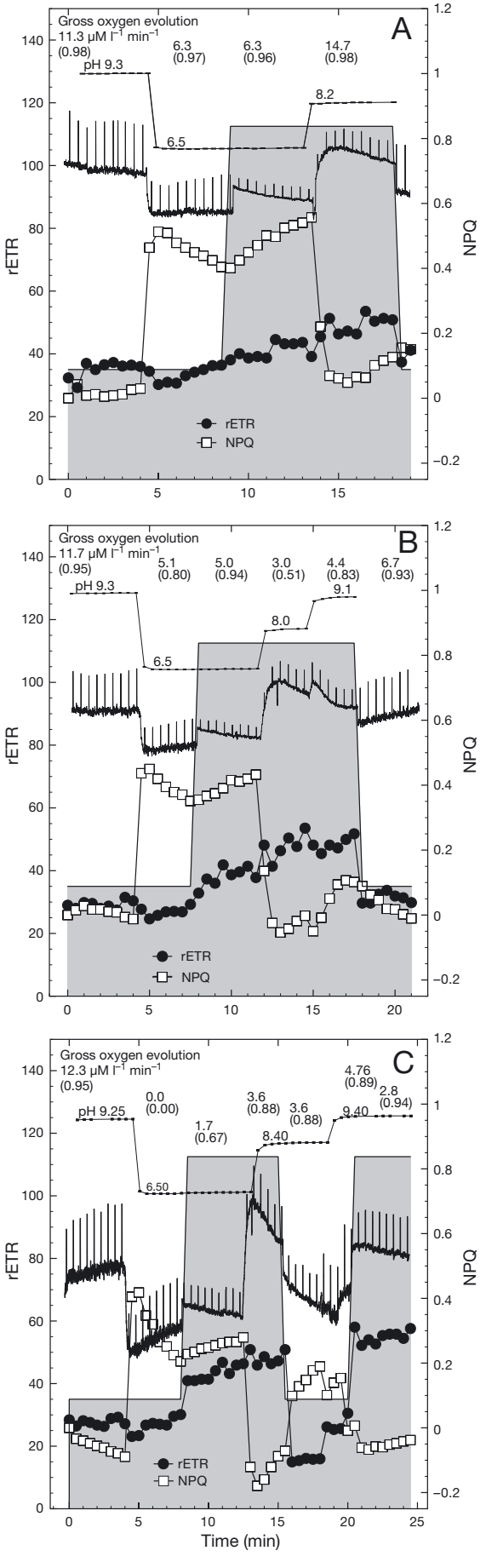

Fig. 5. Combined effects of pH perturbance and photon flux on photosynthesis and photoprotection in *Chlorella fusca*. Photon flux was (A) elevated when cells were exposed to acidic conditions and maintained while pH was brought back up again in a single mode, or (B) by 2 consecutive base additions to initial values. The low light relaxation phase was intermitted in (C). Relative electron transport rates (rETR) and photoprotection non-photochemical quenching (NPQ) were determined using variable fluorescence with rETR = $\Delta F/F_m'^{\star}$ photon flux, and NPQ = $(F_m'^{\star} - F_m') / F_m'$, where $F_m'^{\star}$ = the first F_m' value of the experimental protocol. F_m was not measured as cells were not transferred to the dark prior to measurements. For legends and protocol explanations refer to Fig. 4

m^{-2} s^{-1} only caused a minor dip in this 'recovery process'. Interestingly, addition of NaOH caused a slow decrease in σ'_{PSII}. Note that the changes in σ'_{PSII} are generally in the opposite direction to NPQ, as might be expected, but that the kinetics differ.

DISCUSSION

Light intensity stress

Chlorella spp. are known to grow well, even under challenging conditions. In the TLC used in the present study, the cells were exposed to full sunlight for some tens of seconds, then remained for some time in low light (Jerez et al. 2014). This light treatment challenges the photosynthetic apparatus of the cells and requires effective regulation of photosynthesis and photoprotection. Although diatoms perform better than green algae under fluctuating light (Wagner et al. 2006), chlorophyta convert photon energy efficiently to biomass (Wilhelm & Jakob 2011) and are successfully used for mass culture. To test the strain used for high light resistance, we exposed cells continuously to full strength sunlight for an entire day (≤1800 µmol photons m^{-2} s^{-1}, daily irradiance dose ~150 kW m^{-2}). Cells were able to cope with continuous full strength ambient light conditions as shown by fast fluorescence induction curves. Quantum efficiencies and Q_B reduction kinetics were lower in high light, but could recover in the afternoon. Frequently, P phase values were lower than J, which could be caused by a selective operation of the active fluorescence quenchers, or indicate photodamage in PSII. Photodamage impairs Q_A^- reduction kinetics and might lower the degree of Q_B and PQ pool reduction capacities, potentially due to the proximity of Q_B to the susceptible D1 protein (Aro et al. 1993, Jansen et al. 1999). However, the full photosynthetic poten-

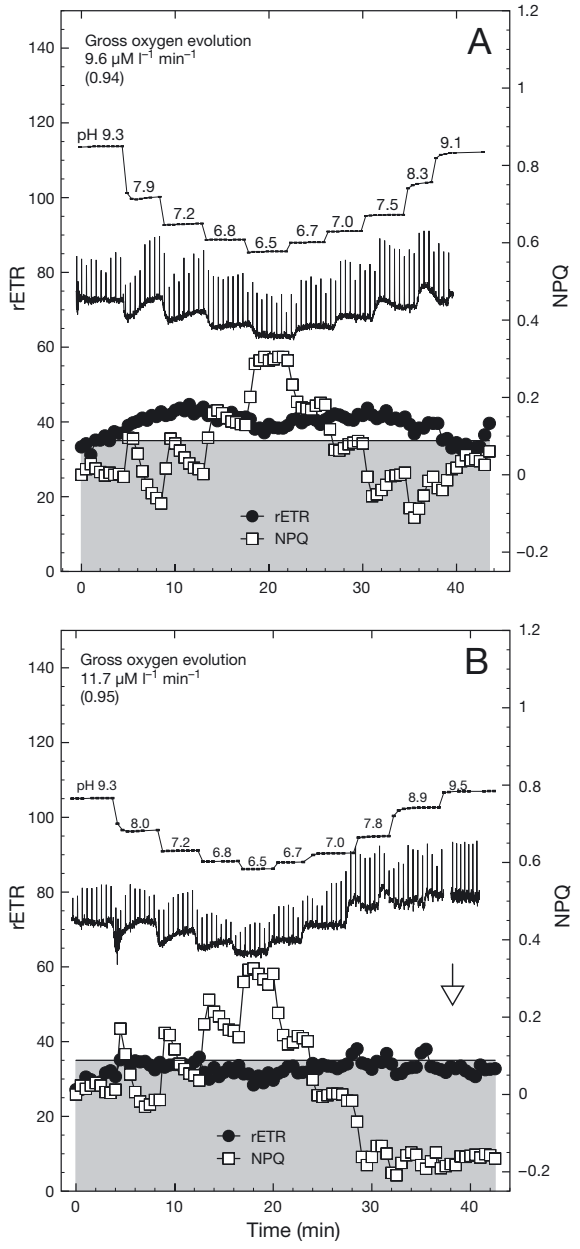

Fig. 6. *Chlorella fusca*. Effects on photosynthesis and photoprotection by consecutive pH adjustments at constant photon flux. (A) and (B) show separate experiments performed on the same day. A DIC addition was performed at the end of (B) (arrow) with a final 0.7 µM

tial could be restored in lower PF in the late afternoon and early evening.

Samples were dark-acclimated only very briefly (≤2 s), which will oxidize primary electron acceptors in PSII (Q_A^-), but not secondary electron acceptors or the PQ pool (Strasser et al. 1995), or relax photoprotective NPQ. Although the rapid phase of energy dependent quenching (q_E) might relax due to a dissipation of the ΔpH-gradient within seconds, xanthophyll cycle-mediated q_E requires minutes, as do state-transitions (Müller et al. 2001, Ihnken et al. 2011a). Residual NPQ in illuminated samples can explain the obvious difference between initial samples, which were dark-acclimated overnight, and samples taken at low PF. Unexpected, however, was that even LL samples showed similar F_v'/F_m' values compared to ML and HL samples in the morning, where the PF at the vessel surface in LL treatments was ≥200 µmol photons m^{-2} s^{-1}. *In situ* rapid light curves showed light saturation at approximately 500 µmol photons m^{-2} s^{-1} (J. C. Kromkamp pers. comm.), which indicates that LL cells were light-limited except for the highest PF at noon. Interesting, even LL samples appear to be photoinhibited around noon and needed to repair in the afternoon, as shown by a lag of F_v'/F_m' up-regulation after the highest light values in the diurnal cycle. Theoretically, chlorophyta perform better under continuous PF (as provided in the PF experiment) compared to fluctuating light (in the TLC) (Wagner et al. 2006), but *Chlorella* cells can acclimate to various, and fluctuating, PF regimes without compromising growth (Kroon et al. 1992a,b), or be stimulated by fluctuating light compared to continuous light exposure (Wijanarko et al. 2007). However, it is possible that a change in the light exposure treatment affected the photosynthetic performance in the present study. Cells experienced fluctuating light under growth conditions in the TLC and were then exposed to continuous PF for 1 d in the PF experiment. Photoacclimation may take hours to days, and is an energy-dependent process (Post et al. 1984, Wilhelm & Wild 1984, Havelkova-Dousova et al. 2004). It is possible that LL samples needed longer to adjust to the changed PF regime due to lower energy capture compared to ML and HL. However, LL conditions in pH drift experiments did not restrain pH drift, which shows that cells were still able to perform well, at least when the initial pH was high (Fig. 1B).

Generally, cells were resistant to severe photo-damage due to effective repair, or efficient and progressive photoprotection. These results show that cells were able to cope with *in situ*, and partly very high, PF without major damage. The very restricted pH drift at pH ~7 was therefore not due to impairment of the photosynthetic machinery.

pH or DIC effects?

pH drift experiments showed very low activity at approximately pH 7.2. The low photosynthetic activity at this pH is surprising, as *Chlorella* sp. showed

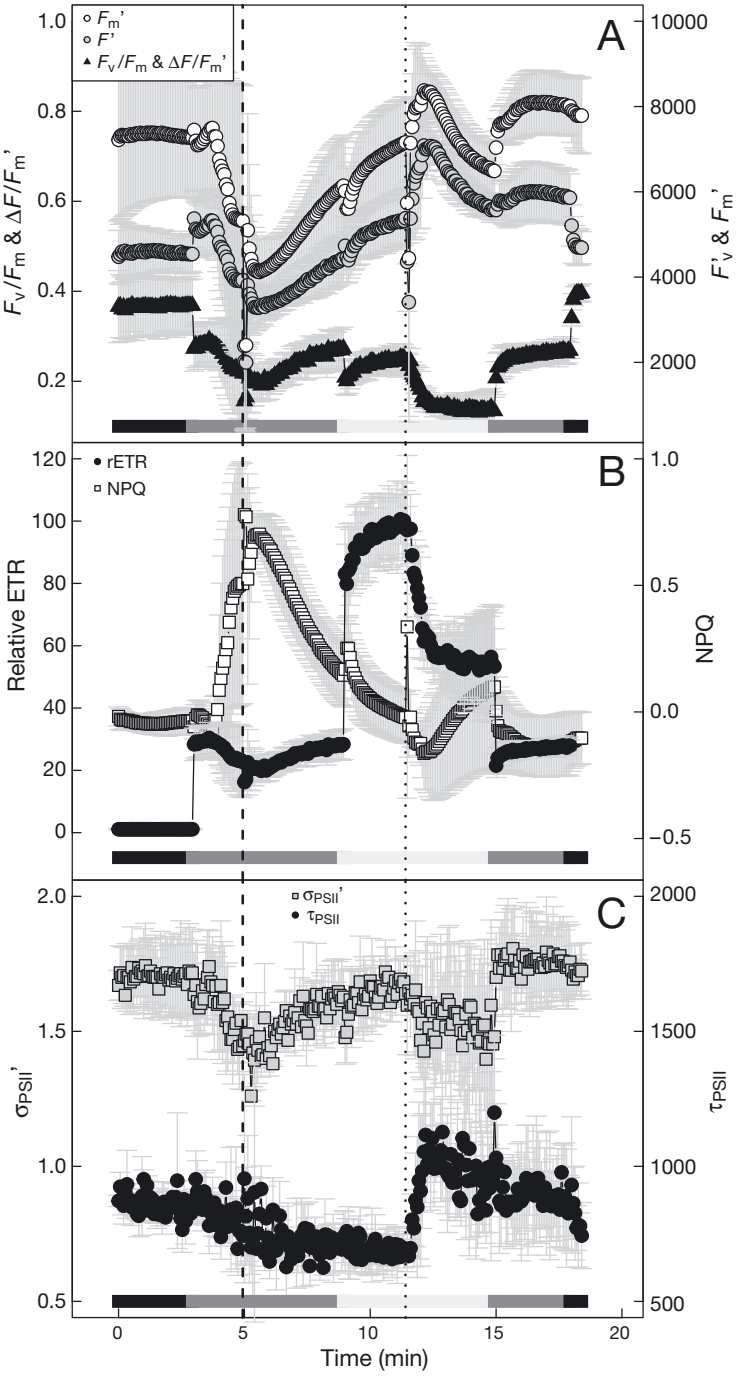

Fig. 7. *Chlorella fusca*. Fluorescence parameters measured by FRRf in response to manipulated pH and actinic light conditions. High initial pH (9.3) was lowered by addition of HCL (dashed line) to a theoretical pH 6.5. After 5 min, the cell solution was alkalized by injection of NaOH (dotted line) to a theoretical pH 8.5. Grey scale bars indicate actinic photon flux: 3, 140, 400 and 0 µmol photons m^{-2} s^{-1}. Data in (A) show minimal fluorescence in darkness or actinic light (F), maximal fluorescence during a single turnover flashlet application (F_m') and effective (or maximal) quantum yields; (B) shows relative electron transport rates (rETR) and non-photochemical quenching (NPQ). The iterative curve fit during the single turnover fluorescence emission allows determination of the functional absorption cross-section of PSII (σ_{PSII}); (C) Re-oxidation kinetics of Q_A^- after the single turnover are shown by τ_{PSII}. Data show mean ± SD for n = 3

highest growth rates at pH 7 or lower (Myers 1953, Goldman et al. 1982), and can raise the pH to values well over pH 10 (Myers 1953) due to the presence of efficient CCMs and bicarbonate uptake capacity (Shelp & Canvin 1980, Beardall 1981, Beardall & Raven 1981). We were not able to measure the DIC concentration, but suspected a DIC limitation when the pH was low. At an acidic pH, the total DIC concentration is much lower than at an alkaline pH. At pH 7.0, for instance, [DIC] = 74 µM, while at pH 9.0 [DIC] = 6300 µM when solutions are in air equilibrium (temperature = 25°C, salinity = 0), calculated using R; (R Development Core Team 2013) package seacarb 3.0 (Lavigne & Gattuso 2011). The *in situ* DIC concentrations would have been much higher because cell suspensions were maintained at pH ~7.2 by aeration with CO_2 gas. DIC addition experiments did not stimulate pH drift, nor rETR. The DIC additions were sufficiently substantial to enable photosynthesis for several hours if DIC would have been limiting (gross O_2 production ~10 µM l^{-1} min^{-1} ≈ CO_2 consumption; DIC additions 400, 800 mM). We therefore concluded that the DIC concentration was not restricting photosynthesis in the TLC, or in pH drift experiments. After the pH was raised by bicarbonate addition in the TLC, pH drift was stimulated. Final pH values were high and showed substantial DIC acquisition and photosynthetic capacity compared to other studies and species (Merrett et al. 1996, Choo et al. 2002, Ihnken et al. 2011b). An increase in pH also elevated growth in a *Chlorella* mass-culture (Castrillo et al. 2013). Similar conclusions were made using marine algae *in situ*. The H^+ concentration, and not the DIC concentration, was the primary factor for cell regulation, growth and photosynthesis in moderate pH manipulation experiments (Lundholm et al. 2005, Hansen et al. 2007, Middelboe & Hansen 2007). Unfortunately, it is not clear what drives these effects due to the complexity of pH and inter-relationships with different cell functions (Smith & Raven 1979, Felle 2001). However, it can be concluded that impaired pH drift was neither due to DIC limitation, nor to PF effects in the present study.

pH-dependent acclimation patterns

O_2 evolution was repressed when the pH was decreased from alkaline conditions to pH 6.5.

Cells grown at various pH levels show species-dependent pH effects (Schneider et al. 2013). Cyanobacteria growth was depressed by acidification (Wang et al. 2011), while seagrass photosynthesis decreased with increasing pH (Invers et al. 1997). Unfavorable pH conditions increased dark respiration and repressed photosynthetic activity in *Euglena* (Danilov & Ekelund 2001) and cyanobacteria, while F_v/F_m was not affected by pH (Liao et al. 2006).

It was expected that a pH increase would be less favored by *Chlorella*. Alkaline conditions increase the likelihood of cell damage due to increased concentrations of reactive oxygen species at high pH (Liu et al. 2007). At pH 7, internal pH values are similar to the external medium (Smith & Raven 1979, Beardall & Raven 1981, Gehl & Colman 1985, Sianoudis et al. 1987), which suggests an energetic advantage at this pH due to low costs for homeostasis. Proton regulation can be energetically expensive (Smith & Raven 1979, Briskin & Hanson 1992) and involve regulative ATPase activity (Weiss & Pick 1996). Active proton pumping might only be employed by the cell during short-term regulation (Bethmann & Schönknecht 2009), while steady-state homeostasis might be facilitated mainly by anion exchange (Lew 2010) in *Chlorella fusca* by a K^+/H^+ antiport system (Tromballa 1987).

However, the substantial pH perturbations in the present study were carried out in a shock-mode, which is likely to require active H^+ pumping and entail ATP consumption (Bethmann & Schönknecht 2009). Because the intra-cellular pH could not be determined, it is not clear if (and how fast) homeostasis was reached. Photoautotrophic cells can regulate internal pH in time scales of minutes (Bethmann & Schönknecht 2009), but no information of rapid internal pH regulations (in seconds) was found in the literature for *Chlorella*. Limitations of internal pH maintenance requires extreme external pH (Gehl & Colman 1985), or osmotic stress (Goyal & Gimmler 1989) and induced internal pH changes of approximately 0.9 and 0.15 units respectively. F', and F_m' values related positively with pH in the present study: the higher the pH, the higher the fluorescence signal. NPQ was activated by acidification. Similar results have been found for thylakoid fragments (Rees et al. 1992, Heinze & Dau 1996). In these studies, fluorescence responded in seconds, and a steady-state was reached within 1 min. These results can be explained by the quenching of the NPQ component q_E, which was directly triggered by pH, irrespective of photosynthetic ETR. A lumen pH of 6 clearly activates q_E (Kramer et al. 1999). Similarly, Jajoo et al. (2012) showed that pH changes can induce a thylakoid membrane re-organisation in pea thylakoid membranes. However, in the present study intact cells were used, and cell compartment membranes as well as pH regulatory mechanisms are expected to regulate internal pH effectively. If external pH perturbation could affect q_E directly, the cells' pH regulation would be severely impaired. The exponential growth phase was passed in the TLC, which is very likely to have lowered the cell fitness. Cells in the stationary phase show distinctively different genetic activity, photophysiological characteristics (Humby et al. 2013) and are more susceptible to external stress factors (Randhawa et al. 2013). However, senescence effects are under-investigated (Humby et al. 2013). It appears likely that cells exploit alternative electron transport routes to increase energy dissipation to compensate for decreased photosynthetic energy quenching capacity. During ionic stress in higher plants, electron acceptance at the plastid terminal oxidase site (PTOX) accounted for up to 30% of the electron transport in PSII (Stepien & Johnson 2009). Because PTOX activity consumes oxygen while electron transport is facilitated, this mechanism could explain the discrepancy between rETR and gross oxygen evolution in the present study. Electrons are being transported and donated to molecular oxygen at the PTOX, with water as an end product (Kuntz 2004, Cardol et al. 2011). However, increasing, not decreasing, pH supported PTOX-mediated O_2 consumption (Josse et al. 2003), i.e. reaction kinetics operate in the opposite direction and are therefore not likely to explain low oxygen evolution rates in acidified samples in the present study. It is still unknown if PTOX activity can generally act as a safety valve under stress conditions in higher plants, partly due to open questions regarding reduction kinetics in this pathway (Trouillard et al. 2012, Laureau et al. 2013). Nevertheless, it is possible that this mechanism is employed under pH shock conditions in *Chlorella* as electron redox systems can participate in homeostasis (Houyoux et al. 2011).

A segregation between ETR and oxygenetic photosynthesis can be explained by state-transitions (Ihnken et al. 2014). Further studies must evaluate if state-transitions occur in *Chlorella* under conditions of pH stress and test the hypothesis that q_T is the reason for changes in variable fluorescence readings and the seeming segregation of rETR and O_2 evolution. A deviation from ETR/O_2 photosynthesis linearity can also be explained by other mechanisms, such as cyclic electron flow around PSII. Cyclic electron transport in PSII suggests photosynthetic electron transport, but electrons are cycled within PSII and do

not contribute to photosynthesis. Alternatively, nitrate reduction, elevated oxygen consuming processes such as the Mehler reaction (Asada 2000, Heber 2002), photorespiraton/chlororespiration (Beardall et al. 2003, Peterhansel & Maurino 2011) or mitochondrial respiration can cause deviation between fluorescence and oxygen based measurements.

A pH effect on the inter-PS-system redox chain was clearly shown in the present study. Q_A^- re-oxidation kinetics (τ_{PSII}; Fig. 7C) increased with alkalization. Faster Q_A^- re-oxidation, most likely due to a higher oxidation state of the PQ pool, was not facilitated by elevated electron transport, as rETR decreased when the base was added. This clearly shows that alternative electron routes are employed by the cells when the pH of the external medium is perturbed. However, rapid alkalization causes cells to aggregate temporarily (Castrillo et al. 2013), which can cause self-shading similar to the package-effect (Berner et al. 1989). It is therefore possible that high τ_{PSII} values are artifacts caused by cell aggregation after addition of the alkaline solution.

DIC acquisition

Costs for DIC acquisition are expected to be lower at pH 6.5 due to the higher CO_2:HCO_3^- ratio compared to pH 9.5. *Chlorella* possesses effective CCMs and can actively acquire both CO_2 and HCO_3^- (Shelp & Canvin 1980, Beardall 1981, Beardall & Raven 1981, Matsuda & Colman 1995a,b). Predominantly, bicarbonate CCMs are anion transporters which can operate as symport or antiport systems using Na^+ (Badger et al. 2002) or Cl^- (Young et al. 2001). Because anion regulation is also involved in homeostasis, HCO_3^- acquisition and consumption might be related to internal pH regulation. Cells acclimated to alkaline pH might combine bicarbonate acquisition and pH regulation, although uptake of HCO_3^- does not appear preferable as bicarbonate must dissociate to CO_2 (which is fixed in the Calvin-Benson-Bassham-cycle) and OH^- (which hydrolyses to water under 'consumption' of H^+). Nevertheless, cells exhibited higher photosynthetic rates at alkaline pH compared to measurements taken at pH 6.5. Compared to optimal growth conditions, RuBisCO contents are down-regulated when cells enter the stationary growth phase (Humby et al. 2013). A CCM up-regulation can account for low RuBisCO levels (Beardall et al. 1991). If CCM induction is controlled by pH in *Chlorella*, an alkalization might allow higher photosynthetic rates due to CCM up-regulation, or activation.

CONCLUSIONS

The present study shows 2 surprising phenomena. Firstly, cells showed higher performance at elevated pH, a DIC concentration- and light intensity-independent response. As this is in conflict with the majority of the literature values (where *Chlorella* spp. preferred pH ≤ 7), the preconditioning of the cells (having passed the maximal growth phase) is likely to have influenced the outcome of the experiments. The second surprising finding is related to the deviation of oxygen and fluorescence based measurements of photosynthesis. Acidification lowered gross oxygen production, but not electron transport rates in PSII. The reason for this might be related to state-transitions which could not be detected due technical limitations in the present study. Nevertheless, alkalinisation clearly increased the physiological performance of cultures that are not operating at maximum efficiency.

Acknowledgements. The authors express their special gratitude to the local coordinators of the bio-technology workgroup, Irene Malpartida and Roberto Abdala. Special thanks to the Spanish GAP coordinators Félix L. Figueroa and Jesús Mercado, and the Spanish GAP committee María Segovia, Nathalie Korbee, Roberto Abdala, Rafael Conde, Francisca de la Coba, Andreas Reul and Irene Malpartida. Experiments were carried out under support from the Department of Ecology of the Universidad de Málaga. The Netherlands Institute for Sea Research (NIOZ) provided acknowledged travel funds for J.C.K. and S.I. Three anonymous reviewers contributed through constructive criticism.

LITERATURE CITED

Andersen RA, Berges JA, Harrison PF, Watanabe MM (2005) Recipes for freshwater and seawater media. In: Andersen RA (ed) Algal culturing techniques. Elsevier Academic Press, London, p 429–538

Aro EM, McCaffery S, Anderson JM (1993) Photoinhibition and D1 protein degradation in peas acclimated to different growth irradiances. Plant Physiol 103:835–843

Asada K (2000) The water-water cycle as alternative photon and electron sinks. Philos Trans R Soc Lond B Biol Sci 355:1419–1431

Badger MR, Hanson D, Price GD (2002) Evolution and diversity of CO_2 concentrating mechanisms in cyanobacteria. Funct Plant Biol 29:161–173

Beardall J (1981) CO_2 accumulation by *Chlorella saccharophila* (Chlorophyceae) at low external pH: evidence for active transport of inorganic carbon at the chloroplast envelope. J Phycol 17:371–373

Beardall J, Raven JA (1981) Transport of inorganic carbon and the 'CO_2 concentrating mechanism' in *Chlorella emersonii* (Chlorophyceae). J Phycol 17:134–141

Beardall J, Roberts S, Millhouse J (1991) Effects of nitrogen limitation on uptake of inorganic carbon and specific activity of Ribulose-1,5-bisphosphate carboxylase oxygenase in green microalgae. Can J Bot 69:1146–1150

Beardall J, Quigg A, Raven J (2003) Oxygen consumption: photorespiration and chlororespiration. In: Larkum AWD, Douglas SE, Raven JA (eds) Advances in photosynthesis and respiration, Vol 14: photosynthesis in algae. Kluwer Academic Publishers, Dordrecht, p 157–181

Berner T, Dubinsky Z, Wyman K, Falkowski PG (1989) Photoadaptation and the 'package' effect in *Dunaliella tertiolecta* (Chlorophyceae). J Phycol 25:70–78

Bethmann B, Schönknecht G (2009) pH regulation in an acidophilic green alga—a quantitative analysis. New Phytol 183:327–339

Briskin DP, Hanson JB (1992) How does the plant plasma membrane H^+-ATPase pump protons? J Exp Bot 43: 269–289

Bukhov NG, Egorova EA, Govindachary S, Carpentier R (2004) Changes in polyphasic chlorophyll *a* fluorescence induction curve upon inhibition of donor or acceptor side of photosystem II in isolated thylakoids. BBA-Bioenergetics 1657:121–130

Cardol P, Forti G, Finazzi G (2011) Regulation of electron transport in microalgae. BBA-Bioenergetics 1807:912–918

Castrillo M, Lucas-Salas LM, Rodríguez-Gil C, Martínez D (2013) High pH-induced flocculation-sedimentation and effect of supernatant reuse on growth rate and lipid productivity of *Scenedesmus obliquus* and *Chlorella vulgaris*. Bioresour Technol 128:324–329

Choo K, Snoeijs P, Pedersen M (2002) Uptake of inorganic carbon by *Cladophora glomerata* (Chlorophyta) from the Baltic Sea. J Phycol 38:493–502

Danilov RA, Ekelund NGA (2001) Effects of pH on the growth rate, mortality and photosynthesis in *Euglena gracilis*. Folia Microbiol (Praha) 46:549–554

Dixon GK, Brownlee C, Merrett MJ (1989) Measurement of internal pH in the coccolithophore *Emiliania huxleyi* using 2′,7′-bis-(2-carboxyethyl)-5(and-6)carboxyfluorescein acetoxymethylester and digital imaging microscopy. Planta 178:443–449

Felle HH (2001) pH: signal and messenger in plant cells. Plant Biol 3:577–591

Gardner R, Peters P, Peyton B, Cooksey KE (2011) Medium pH and nitrate concentration effects on accumulation of triacylglycerol in two members of the chlorophyta. J Appl Phycol 23:1005–1016

Gehl KA, Colman B (1985) Effect of external pH on the internal pH of *Chlorella saccharophila*. Plant Physiol 77: 917–921

Giordano M, Beardall J, Raven J (2005) CO_2 concentrating mechanisms in algae: mechanisms, environmental modulation, and evolution. Annu Rev Plant Biol 56:99–131

Goldman JC, Azov Y, Riley CB, Dennett MR (1982) The effect of pH in intensive microalgal cultures. I. Biomass regulation. J Exp Mar Biol Ecol 57:1–13

Goyal A, Gimmler H (1989) Osmoregulation in *Dunaliella tertiolecta*: effects of salt stress, and the external pH on the internal pH. Arch Microbiol 152:138–142

Hansen P, Lundholm N, Rost B (2007) Growth limitation in marine red-tide dinoflagellates: effects of pH versus inorganic carbon availability. Mar Ecol Prog Ser 334:63–71

Havelkova-Dousova H, Prášil O, Behrenfeld M (2004) Photoacclimation of *Dunaliella tertiolecta* (Chlorophyceae) under fluctuating irradiance. Photosynthetica 42:273–281

Heber U (2002) Irrungen, Wirrungen? The Mehler reaction in relation to cyclic electron transport in C3 plants. Photosynth Res 73:223–231

Heinze I, Dau H (1996) The pH-dependence of the photosystem II fluorescence: cooperative transition to a quenching state. Ber Bunsenges Phys Chem 100:2008–2013

Hinga KR (2002) Effects of pH on coastal marine phytoplankton. Mar Ecol Prog Ser 238:281–300

Houyoux PA, Ghysels B, Lecler R, Franck F (2011) Interplay between non-photochemical plastoquinone reduction and re-oxidation in pre-illuminated *Chlamydomonas reinhardtii*: a chlorophyll fluorescence study. Photosynth Res 110:13–24

Humby PL, Snyder ECR, Durnford DG (2013) Conditional senescence in *Chlamydomonas reinhardtii* (Chlorophyceae). J Phycol 49:389–400

Ihnken S, Kromkamp JC, Beardall J (2011a) Photoacclimation in *Dunaliella tertiolecta* reveals a unique NPQ pattern upon exposure to irradiance. Photosynth Res 110:123–137

Ihnken S, Roberts S, Beardall J (2011b) Differential responses of growth and photosynthesis in the marine diatom *Chaetoceros muelleri* to CO_2 and light availability. Phycologia 50:182–193

Ihnken S, Kromkamp JC, Beardall J, Silsbe GM (2014) State-transitions facilitate robust quantum yields and cause an over-estimation of electron transport in *Dunaliella tertiolecta* cells held at the CO_2 compensation point and re-supplied with DIC. Photosynth Res 119:257–272

Invers O, Romero J, Pérez M (1997) Effects of pH on seagrass photosynthesis: a laboratory and field assessment. Aquat Bot 59:185–194

Jacobsen A, Grahl-Nielsen O, Magnesen T (2010) Does a large-scale continuous algal production system provide a stable supply of fatty acids to bivalve hatcheries? J Appl Phycol 22:769–777

Jajoo A, Szabó M, Zsiros O, Garab G (2012) Low pH induced structural reorganization in thylakoid membranes. Biochim Biophys Acta 1817:1388–1391

Jansen MA, Mattoo AK, Edelman M (1999) D1-D2 protein degradation in the chloroplast. Eur J Biochem 260: 527–532

Jerez CG, Navarro E, Malpartida I, Rico RM, Masojídek J, Abdala R, Figueroa FL (2014) Hydrodynamics and photosynthesis performance of *Chlorella fusca* grown in a thin-layer cascade (TLC) system. Aquat Biol 22:111–122

Josse EM, Alcaraz JP, Labouré AM, Kuntz M (2003) *In vitro* characterization of a plastid terminal oxidase (PTOX). Eur J Biochem 270:3787–3794

Kolber Z, Falkowski PG (1992) Fast repetition rate (FRR) fluorometer for making *in situ* measurements of primary productivity. In: OCEANS'92. Mastering the Oceans Through Technology. Vol 2. IEEE, New York, NY, p 637–641

Kolber Z, Falkowski PG (1993) Use of active fluorescence to estimate phytoplankton photosynthesis in situ. Limnol Oceanogr 38:1646–1665

Kolber ZS, Prasil O, Falkowski PG (1998) Measurements of variable chlorophyll fluorescence using fast repetition rate techniques: defining methodology and experimental protocols. BBA-Bioenergetics 1367:88–106

Kramer D, Sacksteder C, Cruz J (1999) How acidic is the lumen? Photosynth Res 60:151–163

Kromkamp J, Forster R (2003) The use of variable fluorescence measurements in aquatic ecosystems: differences between multiple and single turnover measuring protocols and suggested terminology. Eur J Phycol 38:103–112

Kroon B, Burgerwiersma T, Visser P, Mur L (1992a) The effect of dynamic light regimes on *Chlorella*. 2: Minimum quantum requirement and photosynthesis-irradiance parameters. Hydrobiologia 238:79–88

Kroon B, Latasa M, Ibelings B, Mur L (1992b) The effect of dynamic light regimes on *Chlorella*. 1: pigments and cross-sections. Hydrobiologia 238:71–78

Kuntz M (2004) Plastid terminal oxidase and its biological significance. Planta 218:896–899

Kurkdjian A, Guern J (1989) Intracellular pH: measurement and importance in cell activity. Annu Rev Plant Biol 40: 271–303

Laureau C, Paepe RD, Latouche G, Moreno Chacón M and others (2013) Plastid terminal oxidase (PTOX) has the potential to act as a safety valve for excess excitation energy in the alpine plant species *Ranunculus glacialis* L. Plant Cell Environ 36:1296–1310

Lavigne H, Gattuso JP (2011) Seacarb: seawater carbonate chemistry with R. R package version 2.4.2. http://CRAN.R-project.org/package=seacarb

Lew RR (2010) Ion and oxygen fluxes in the unicellular alga *Eremosphaera viridis*. Plant Cell Physiol 51:1889–1899

Liao CC, Liu SL, Wang WL (2006) Effects of temperature and pH on growth and photosynthesis of the thermophilic cyanobacterium *Synechococcus lividus* as measured by pulse-amplitude modulated fluorometry. Phycological Res 54:260–268

Liu W, Au D, Anderson D, Lam P, Wu R (2007) Effects of nutrients, salinity, pH and light:dark cycle on the production of reactive oxygen species in the alga *Chattonella marina*. J Exp Mar Biol Ecol 346:76–86

Liu J, Mukherjee J, Hawkes JJ, Wilkinson SJ (2013) Optimization of lipid production for algal biodiesel in nitrogen stressed cells of *Dunaliella salina* using FTIR analysis. J Chem Technol Biotechnol 88:1807–1814

Lundholm N, Hansen P, Kotaki Y (2004) Effect of pH on growth and domoic acid production by potentially toxic diatoms of the genera *Pseudo-nitzschia* and *Nitzschia*. Mar Ecol Prog Ser 273:1–15

Lundholm N, Hansen PJ, Kotaki Y (2005) Lack of allelopathic effects of the domoic acid-producing marine diatom *Pseudo-nitzschia multiseries*. Mar Ecol Prog Ser 288:21–33

Matsuda Y, Colman B (1995a) Induction of CO_2 and bicarbonate transport in the green alga *Chlorella ellipsoidea* (II. Evidence for induction in response to external CO_2 concentration). Plant Physiol 108:253–260

Matsuda Y, Colman B (1995b) Induction of CO_2 and bicarbonate transport in the green alga *Chlorella ellipsoidea* (I. Time course of induction of the two systems). Plant Physiol 108:247–252

Merrett M, Nimer NA, Dong L (1996) The utilization of bicarbonate ions by the marine microalga *Nannochloropsis oculata* (Droop) Hibberd. Plant Cell Environ 19:478–484

Middelboe AL, Hansen PJ (2007) Direct effects of pH and inorganic carbon on macroalgal photosynthesis and growth. Mar Biol Res 3:134–144

Müller P, Li XP, Niyogi KK (2001) Non-photochemical quenching. A response to excess light energy. Plant Physiol 125:1558–1566

Myers J (1953) Growth characteristics of algae in relation to the problems of mass culture. In: Burlew JS (ed) Algal culture: from laboratory to pilot plant. Carnegie Institution of Washington, Publication no. 600, Washington, DC, p 37–54

Nielsen LT, Lundholm N, Hansen PJ (2007) Does irradiance influence the tolerance of marine phytoplankton to high pH? Mar Biol Res 3:446–453

Peterhansel C, Maurino VG (2011) Photorespiration redesigned. Plant Physiol 155:49–55

Post A, Dubinsky Z, Wyman K, Falkowski P (1984) Kinetics of light-intensity adaptation in a marine planktonic diatom. Mar Biol 83:231–238

R Development Core Team (2013) R: a language and environment for statistical computing. R foundation for statistical computing, Vienna

Randhawa V, Thakkar M, Wei L (2013) Effect of algal growth phase on *Aureococcus anophagefferens* susceptibility to hydrogen peroxide. Aquat Toxicol 142-143: 230–238

Rees D, Noctor G, Ruban A, Crofts J, Young A, Horton P (1992) pH dependent chlorophyll fluorescence quenching in spinach thylakoids from light treated or dark adapted leaves. Photosynth Res 31:11–19

Schneider SC, Kahlert M, Kelly MG (2013) Interactions between pH and nutrients on benthic algae in streams and consequences for ecological status assessment and species richness patterns. Sci Total Environ 444:73–84

Shelp BJ, Canvin DT (1980) Utilization of exogenous inorganic carbon species in photosynthesis by *Chlorella pyrenoidosa*. Plant Physiol 65:774–779

Sianoudis J, Küsel AC, Mayer A, Grimme LH, Leibfritz D (1987) The cytoplasmic pH in photosynthesizing cells of the green alga *Chlorella fusca*, measured by P-31 NMR spectroscopy. Arch Microbiol 147:25–29

Smith FA, Raven JA (1979) Intracellular pH and its regulation. Annu Rev Plant Physiol 30:289–311

Stepien P, Johnson GN (2009) Contrasting responses of photosynthesis to salt stress in the glycophyte Arabidopsis and the halophyte Thellungiella: role of the plastid terminal oxidase as an alternative electron sink. Plant Physiol 149:1154–1165

Stirbet A, Govindjee (2012) Chlorophyll *a* fluorescence induction: a personal perspective of the thermal phase, the J–I–P rise. Photosynth Res 113:15–61

Strasser RJ, Srivastava A, Govindjee (1995) Polyphasic chlorophyll *a* fluorescence transient in plants and cyanobacteria. Photochem Photobiol 61:32–42

Taraldsvik M, Mykleastad S (2000) The effect on growth rate, biochemical composition and extracellular carbohydrate production of the marine diatom *Skeletonema costatum*. Eur J Phycol 35:189–194

Tomek P, Lazár D, Ilík P, Nauš J (2001) On the intermediate steps between the O and P steps in chlorophyll *a* fluorescence rise measured at different intensities of exciting light. Aust J Plant Physiol 28:1151–1160

Tóth SZ, Schansker G, Strasser RJ (2005) Intact leaves, the maximum fluorescence level (F-M) is independent of the redox state of the plastoquinone pool: A DCMU-inhibition study. BBA-Bioenergetics 1708:275–282

Tóth SZ, Schansker G, Strasser RJ (2007) A non-invasive assay of the plastoquinone pool redox state based on the OJIP-transient. Photosynth Res 93:193–203

Tromballa HW (1987) Base uptake, K^+ transport and intracellular pH regulation by the green alga *Chlorella fusca*. Biochim Biophys Acta 904:216–226

Trouillard M, Shahbazi M, Moyet L, Rappaport F, Joliot P, Kuntz M, Finazzi G (2012) Kinetic properties and physiological role of the plastoquinone terminal oxidase (PTOX) in a vascular plant. Biochim Biophys Acta 1817: 2140–2148

van Kooten O, Snel JFH (1990) The use of chlorophyll fluorescence nomenclature in plant stress physiology. Photosynth Res 25:147–150

Wagner H, Jakob T, Wilhelm C (2006) Balancing the energy flow from captured light to biomass under fluctuating light conditions. New Phytol 169:95–108

Wang X, Hao C, Zhang F, Feng C, Yang Y (2011) Inhibition of the growth of two blue-green algae species (*Microsystis aruginosa* and *Anabaena spiroides*) by acidification treatments using carbon dioxide. Bioresour Technol 102:

5742–5748

Weiss M, Pick U (1996) Primary structure and effect of pH on the expression of the plasma membrane H^+-ATPase from *Dunaliella acidophila* and *Dunaliella salina*. Plant Physiol 112:1693–1702

Wijanarko A, Sendjaya DAY, Gozan M, Soemantojo RW, Witarto AB, Ohtaguchi KAK (2007) Enhanced *Chlorella vulgaris* (Buitenzorg) growth by photon flux density alteration in serial bubble column photobioreactors. ASEAN J Chem Eng 7:89–101

Wilhelm C, Jakob T (2011) From photons to biomass and biofuels: evaluation of different strategies for the improvement of algal biotechnology based on comparative energy balances. Appl Microbiol Biotechnol 92: 909–919

Wilhelm C, Wild A (1984) The variability of the photosynthetic unit in *Chlorella*. II: The effect of light intensity and cell development on photosynthesis, P-700 and cytochrome f in homocontinuous and synchronous cultures of *Chlorella*. J Plant Physiol 115:125–135

Young E, Beardall J, Giordano M (2001) Inorganic carbon acquisition by *Dunaliella tertiolecta* (Chlorophyta) involves external carbonic anhydrase and direct HCO_3^- utilization insensitive to the anion exchange inhibitor DIDS. Eur J Phycol 36:81–88

Zhu XG, Govindjee, Baker NR, deSturler E, Ort DR, Long SP (2005) Chlorophyll *a* fluorescence induction kinetics in leaves predicted from a model describing each discrete step of excitation energy and electron transfer associated with Photosystem II. Planta 223:114–133

Appendix.

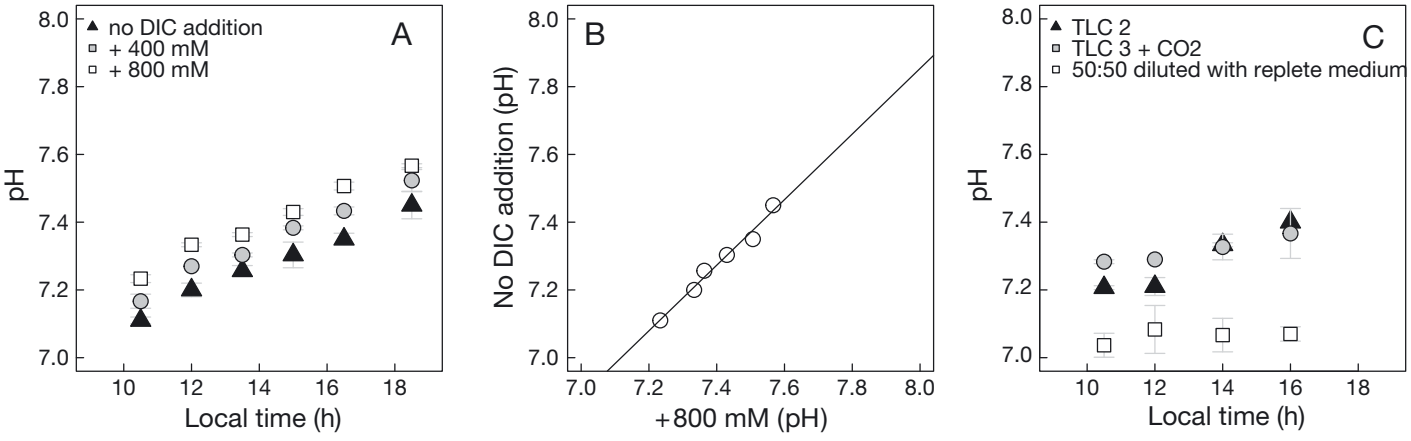

Fig. A1. pH drift experiments. (A) Cells were supplemented with $NaHCO_3^-$; (B) shows a scatter plot of (A) for samples without DIC amendment and samples where an 800 mM bicarbonate supplement was performed. (C) Shows additional pH drift experiments from TLC2 and TLC3, where cell suspensions were bubbled with CO_2 prior to pH drift experiments, and samples that were diluted with fresh, nutrient replete medium (50:50 by volume). Data are mean ± SD (n = 3)

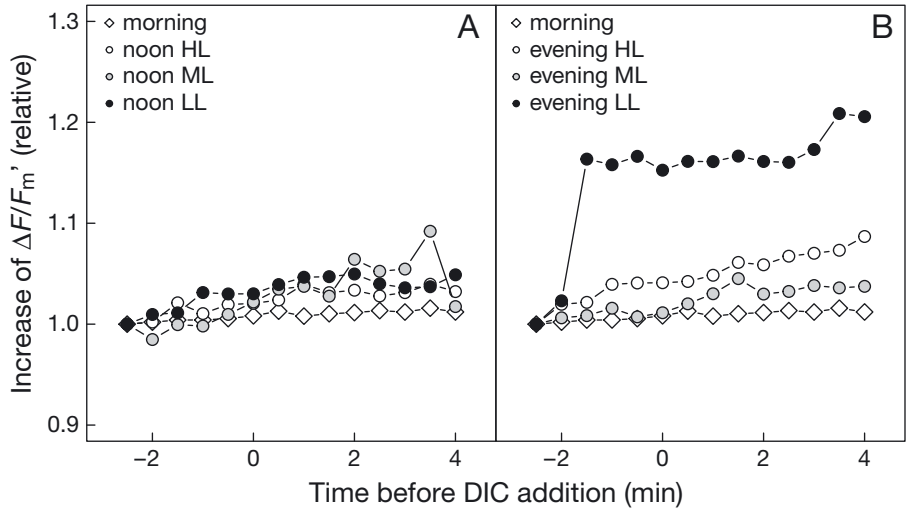

Fig. A2. Samples of the photon flux (PF) experiment (see Figs. 2 & 3) were withdrawn, exposed to a constant PF of 140 µmol photons m^{-2} s^{-1} and supplemented with 300 µM dissolved inorganic carbon (DIC) at t = 0 min, while $\varnothing F/F_m'$ values were recorded every 30 s. Data were normalized to the first value. Data show mean (n = 3), SD were omitted for readability but rarely exceeded 5% with the exception of evening light limitation (LL) samples, where 20% SD were common

Submitted: December 2, 2013; Accepted: June 20, 2014 *Proofs received from author(s): August 22, 2014*